

Can the Delay in Antarctic Polar Vortex Breakup Explain Recent Trends in Surface Westerlies?

ADITI SHESHADRI AND R. ALAN PLUMB

Department of Earth, Atmospheric and Planetary Sciences, Massachusetts Institute of Technology, Cambridge, Massachusetts

DANIELA I. V. DOMEISEN*

Department of Earth and Atmospheric Sciences, Cornell University, Ithaca, New York

(Manuscript received 12 December 2012, in final form 18 October 2013)

ABSTRACT

The authors test the hypothesis that recent observed trends in surface westerlies in the Southern Hemisphere are directly consequent on observed trends in the timing of stratospheric final warming events. The analysis begins by verifying that final warming events have an impact on tropospheric circulation in a simplified GCM driven by specified equilibrium temperature distributions. Seasonal variations are imposed in the stratosphere only. The model produces qualitatively realistic final warming events whose influence extends down to the surface, much like what has been reported in observational analyses. The authors then go on to study observed trends in surface westerlies composited with respect to the date of final warming events. If the considered hypothesis were correct, these trends would appear to be much weaker when composited with respect to the date of the final warming events. The authors find that this is not the case, and accordingly they conclude that the observed surface changes cannot be attributed simply to this shift toward later final warming events.

1. Introduction

In both hemispheres, stratospheric polar vortices form in the fall, reach maximum strength in midwinter, and decay in late winter–spring. The breakdown of these vortices is known as the stratospheric final warming (SFW). Observational and modeling evidence suggests that fluctuations in the polar stratospheric vortices in both hemispheres have an effect on the troposphere (e.g., Baldwin and Dunkerton 2001; Thompson and Solomon 2002; Polvani and Kushner 2002; Gillett and Thompson 2003). Various studies linking the strength of the Northern Hemisphere winter stratospheric polar vortex to tropospheric climate (e.g., Baldwin and Dunkerton 2001; Thompson and Wallace 2000; Thompson et al. 2005) indicate that a stronger stratospheric polar vortex is

associated with stronger tropospheric westerlies in the vicinity of 60°N.

Black et al. (2006) in their exploratory study of SFW events in the Northern Hemisphere reported that these events provide a strong organizing influence upon the large-scale circulation of the stratosphere and troposphere during the period of spring onset and Black and McDaniel (2007a) studied the dynamics of these events in the Northern Hemisphere. Black and McDaniel (2007b) investigated the organizing influence of SFW events on the circulation of the Southern Hemisphere. They found that part of the annual weakening of the high-latitude circumpolar westerlies in the uppermost troposphere and stratosphere occurs within a short time surrounding SFW onset and that a coherent annular circulation change occurs during SFW onset with zonal decelerations (accelerations) observed at high (low) latitudes. These studies used reanalysis data and in an attempt to filter out other factors that influence tropospheric circulation and focus on the relatively short-term signal around final warming events, considered circulation anomalies from an average seasonal cycle defined by the first six Fourier harmonics. From these studies, it also emerged that the tropospheric circulation response to stratospheric final warming events

* Current affiliation: Institute of Oceanography, University of Hamburg, Hamburg, Germany.

Corresponding author address: Aditi Sheshadri, 54-1515, Department of Earth, Atmospheric and Planetary Sciences, Massachusetts Institute of Technology, 77 Massachusetts Avenue, Cambridge, MA 02139.
E-mail: aditi_s@mit.edu

is structurally distinct from the annular mode in both hemispheres.

A tendency toward an increase in the positive phase of the southern annular mode (SAM) has been reported in the Southern Hemisphere (e.g., Thompson et al. 2000; Fogt et al. 2009). This positive phase of the SAM is associated with a poleward shift of the Southern Hemisphere midlatitude jet and storm tracks (Archer and Caldeira 2008). It has been suggested that stratospheric ozone depletion is the cause of these changes (e.g., Thompson and Solomon 2002; Polvani et al. 2011; Thompson et al. 2011). Polvani et al. (2011) suggest that Southern Hemisphere tropospheric circulation changes in austral summer over the second half of the twentieth century have been caused primarily by polar stratospheric ozone depletion, and, in particular, that ozone depletion leads to a poleward jet shift that extends all the way to the surface. Waugh et al. (1999) and Black and McDaniel (2007b) have noted a trend in the timing of Southern Hemisphere SFW events, with the warming occurring later in recent years. This trend could be a response to the radiative effects of Antarctic ozone depletion (Thompson et al. 2011). Therefore, in this paper we investigate the question of whether the observed changes in surface westerlies could be due to this delay in SFW timing.

We begin our analysis by demonstrating explicitly that stratospheric final warming events have an impact on the troposphere. We do this by investigating final warming events in a simplified general circulation model. In reanalysis data, unambiguous separation of the tropospheric response to stratospheric final warming events from the internal seasonal cycle of the troposphere is difficult. Therefore, we use a model setup that enables the tropospheric response to be attributable explicitly to seasonal changes in the stratosphere. As will be described in section 2, the model is forced by relaxation toward an equilibrium temperature distribution that varies seasonally within the stratosphere but not in the troposphere. Thus, seasonal variations in the tropospheric circulation, including those occurring around the time of the breakdown of the stratospheric polar vortex in spring, are unambiguously stratospheric in origin. In the model configuration used here, a surface topography of zonal wavenumber 2 is included in one hemisphere only in order to force quasi-stationary waves. This makes this hemisphere similar to the observed Northern Hemisphere in its wintertime stratospheric behavior. Even without topography, the model generates enough long-wave activity to make the final warming quite variable in its timing, though it does not produce strong midwinter warming events. We analyze here the model hemisphere with topography. Our interest in this part of the paper is to demonstrate, in a general sense, unambiguous stratospheric

influence on the troposphere during the time of the final warming. It is not intended that the results from this component of the research should be interpreted as being especially applicable to the Southern Hemisphere of the real atmosphere. Our model results in section 2 also resemble that of Black and McDaniel (2007a,b) in that the tropospheric response to final warming events is structurally distinct from the annular mode.

Having demonstrated in section 2 that stratospheric final warming events do impact the circulation of the troposphere, we proceed in section 3 to use National Centers for Environmental Prediction–National Center for Atmospheric Research (NCEP–NCAR) reanalysis data to investigate the question of whether the observed changes in surface westerlies could be due to this delay in SFW timing. To do this, we examine differences between years of large ozone depletion and the pre-ozone-hole years.

2. SFW events in the simplified model

a. Model description

The model that we use is similar to that of Kushner and Polvani (2006). The model is dry and hydrostatic, solving the global primitive equations with T42 resolution in the horizontal and 40 levels in the vertical. Linear damping of the horizontal winds is applied in the planetary boundary layer and in a sponge above 0.5 hPa. The bottom boundary in one hemisphere only includes wave-2 topography [identical to run 9 in Gerber and Polvani (2009)], centered on 45°S and 3000 m high. Newtonian relaxation forces temperatures toward a zonally symmetric equilibrium temperature field T_{eq} . Within the stratosphere, a seasonal cycle in T_{eq} is prescribed using the specification of Kushner and Polvani [2006, their Eqs. (1) and (2)], with the lapse rate fixed at 4 K km⁻¹. This produces a winter stratosphere in the hemisphere with topography that is qualitatively similar to that of the Northern Hemisphere (Gerber and Polvani 2009). Within the troposphere (below 100 hPa), there is no imposed seasonal variation; T_{eq} is specified as in Polvani and Kushner (2002) with the parameter $\varepsilon = -10$ K providing an asymmetry between the Northern and Southern Hemispheres. The equilibrium temperature field varies smoothly from tropospheric to stratospheric specifications across 100 hPa.

b. Model results

We simulated 33 final warmings in the model run. There were 5 years in the model in which sudden warming events occurred that took more than 10 days to recover; these years were excluded from the analysis. Black and McDaniel (2007a), who used NCEP–NCAR reanalysis data to examine SFW events in the Northern

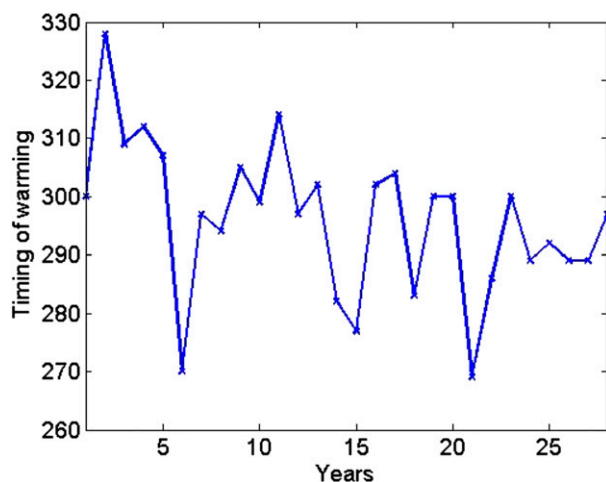


FIG. 1. Timing of SFW events from the 28 years simulated in the model run.

Hemisphere identified SFW events as the final time when the 50-hPa zonal mean zonal wind at 70°N drops below the value of zero without returning to 5 m s^{-1} until the subsequent autumn. The same authors (Black and McDaniel 2007b) used 40-yr European Centre for Medium-Range Weather Forecasts (ECMWF) Re-Analysis (ERA-40) data to analyze Southern Hemisphere SFW events and based their definition for the timing of these events on when the zonal mean zonal wind at 50 hPa and 60°S reached the value of 10 m s^{-1} . The criterion used in this study for the model run was based on the day on which the zonal mean zonal wind at 50 hPa and 60°S reaches the value of 2 m s^{-1} . This yields a final warming date for the model at approximately the same phase of the zonal wind cycle of the model as that used by Black and McDaniel (2007a,b) for the ERA-40 data and the NCEP–NCAR reanalysis data. Varying this definition did not change our results significantly.

Figure 1 shows the timing of SFW events for the 28 years analyzed from the model run. A similar run with no topography does not produce sudden warmings (Gerber and Polvani 2009), but the variability in the timing of final warmings is not profoundly different from the case with topography reported here. The top panel of Fig. 2 shows the zonal mean zonal wind averaged from 60° to 70°S over a 60-day period centered on final warming events and averaged over the 28 years that were analyzed from the simplified GCM run. We see a clear transition from westerlies to easterlies in the stratosphere and a weakening of the westerlies below. The bottom panel of Fig. 2 is similar but presents the time evolution of zonal mean zonal winds averaged from 60° to 70°S relative to day –30. We see from the bottom panel that SFW events in the model have a statistically significant impact that

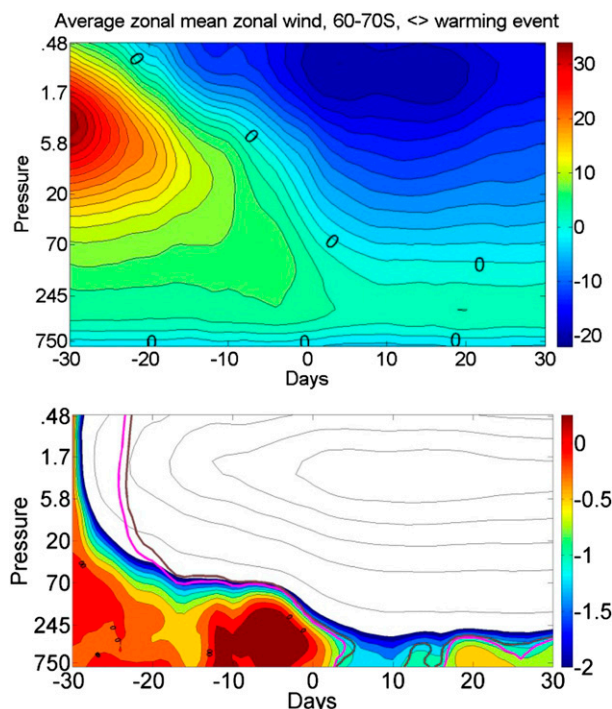


FIG. 2. (top) Transition in zonal mean zonal wind averaged from 60° to 70°S for a 60-day period centered on SFW events for 28 years from the GCM run. The contour interval is 2 m s^{-1} . (bottom) Time evolution of zonal mean zonal wind averaged from 60° to 70°S for a 60-day period centered on SFW events for 28 years from the GCM run as differences from day –30. The contour interval is 0.25 m s^{-1} up to -2 m s^{-1} (filled color contours) and 5 m s^{-1} thereafter (unfilled black contours). Magenta and brown contours denote the 90% and 95% confidence intervals for a two-sided t test.

extends to the surface after day 0. Since there is no imposed seasonal cycle in the troposphere, these surface effects are unambiguously of stratospheric origin. The latitude–pressure structure of the change in zonal mean zonal winds between days +10 and –10 is seen in Fig. 3a. A dipole structure can be seen in the stratosphere, with the winds being decelerated southward of about 40°S. This dipole extends downward into the troposphere and all the way to the surface, in qualitative agreement with the analysis of Black and McDaniel (2007b). Also in agreement with Black and McDaniel (2007b) is the fact that the zonal mean tropospheric wind anomaly, though dipolar, does not match the structure of the model’s annular mode. To illustrate this, we define the model EOF in two ways. In the first, shown in Fig. 3b, we consider the first EOF of zonal mean zonal wind at 585 hPa, which is the first model level above the extent of the topography. This peaks at 23.7° and 36.7°S, whereas the tropospheric dipole in Fig. 3a is displaced significantly poleward of this. The dipole structure in Fig. 3a also does not match the latitude structure of vertically integrated

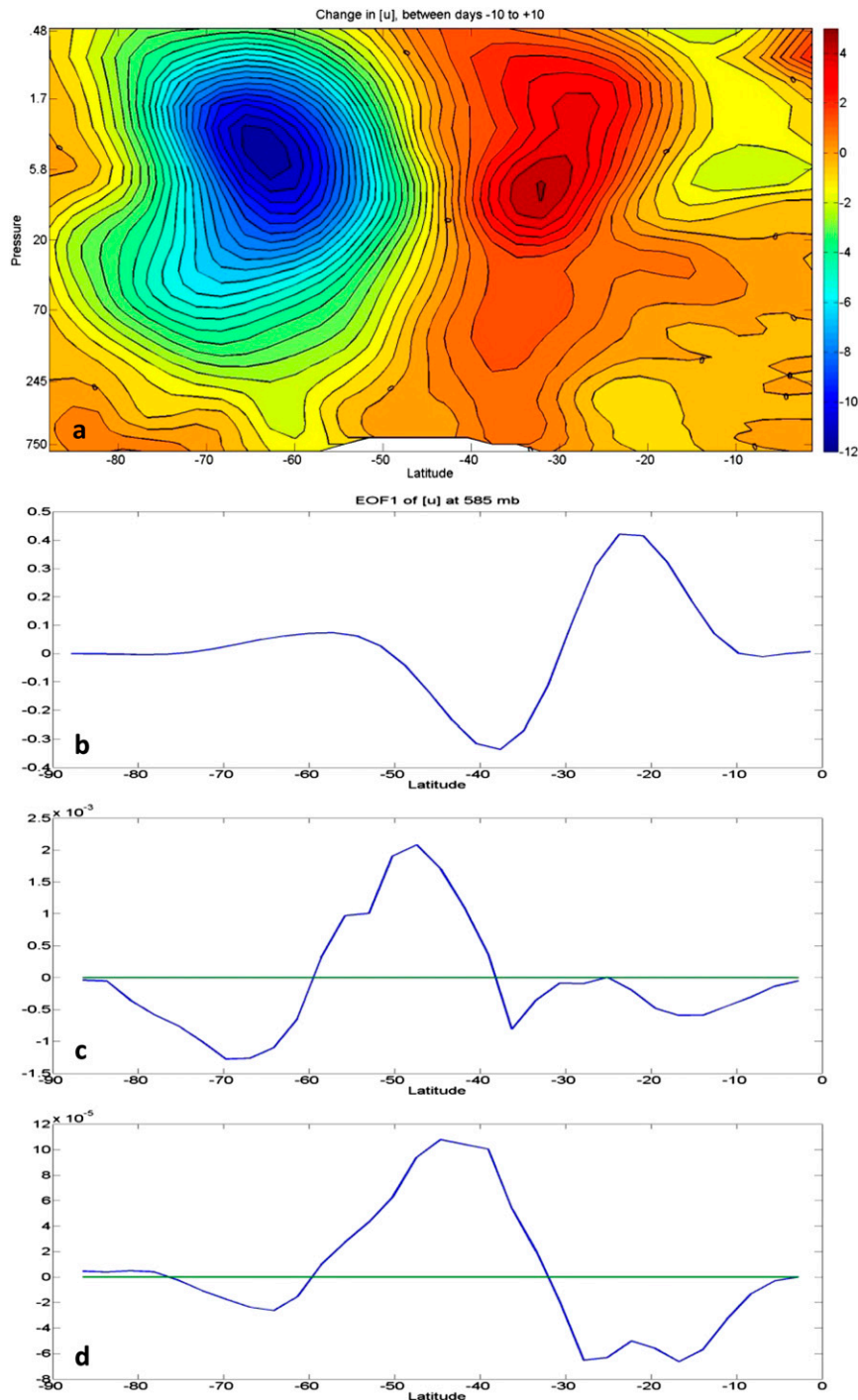


FIG. 3. (a) Latitude–pressure structure of the change in zonal mean zonal winds between days -10 and $+10$. The contour interval is 0.5 m s^{-1} . (b) First EOF of zonal mean zonal winds at 585 hPa. (c) Vertically integrated tropospheric (from the surface to 200 hPa) horizontal momentum flux divergence as anomalies from the climatology averaged over a 21-day period centered on the final warming [same time period as shown in (a)]. (d) Vertically integrated tropospheric (from the surface to 200 hPa) horizontal momentum flux divergence regressed on the first EOF of zonal mean zonal winds at 585 hPa. Plots are from the model run, and the white patch in (a) shows the extent of the bottom topography.

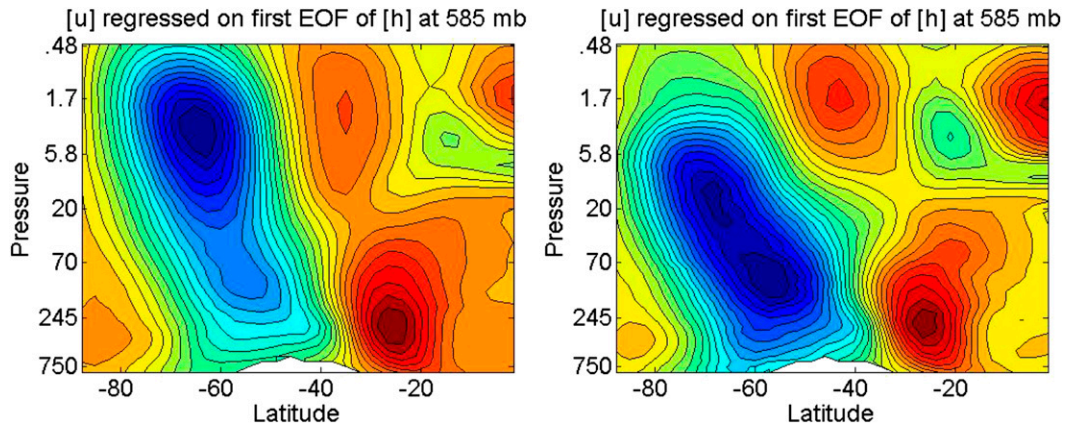


FIG. 4. Latitude–pressure structure of the zonal mean zonal wind regressed on the first EOF of geopotential height at 585 hPa (the first model level above the extent of the topography) for (left) all data and (right) a 90-day period centered on final warming events. Plots are from the model run, and the white patch at the bottom of both figures shows the extent of bottom topography.

anomalous tropospheric (from the surface to 200 hPa) horizontal momentum flux divergence over the same time period (shown in Fig. 3c). Nor does it match the structure of the vertically integrated tropospheric horizontal momentum flux divergence regressed on the first EOF of zonal mean zonal wind at 585 hPa (shown in Fig. 3d). To confirm that this conclusion is not based on this definition of the annular mode, we show in Fig. 4 the structure of zonal mean zonal wind regressed on the principal component time series corresponding to the first EOF of 585-hPa geopotential height. The left panel of Fig. 4 shows the structure of the regression for all data. The right panel shows the structure of the regression using the first EOF of 585 hPa geopotential height computed using springtime data only (a 90-day period centered on the final warming event). By either definition of the annular mode, the tropospheric response to the final warming is shifted poleward of the annular mode. Indeed, the lower-latitude lobe of the dipole of the tropospheric SFW signal (Fig. 3a) almost coincides with the node of the dipole seen in Fig. 4.

3. SFW events in the NCEP–NCAR reanalysis

a. Data and methods

We use daily data from the NCEP–NCAR reanalysis. We study the years 1960–2009, with the exception of 2002, because of the unusual nature of the stratospheric winter in this year (in late September 2002, the Southern Hemisphere underwent its first recorded sudden warming event; e.g., Krüger et al. 2005; Newman and Nash 2005; Baldwin et al. 2003a). We use the term “late years” to refer to the years of large ozone depletion (taken to be 1995–2009, with the exception of 2002) and the term “early

years” to refer to the pre-ozone-hole years (which we take to be 1966–79). The average annual cycle of zonal mean zonal wind at 50 hPa and 60°S had a maximum of 55 m s^{-1} . The criterion for the timing of SFW events was based on the day on which the zonal mean zonal wind at 50 hPa and 60°S reaches the value of 10 m s^{-1} (this is a stage in the vortex breakup that is similar to the 2 m s^{-1} criterion in our model). Again, changing this definition did not affect our results significantly.

b. Results

Figure 5 shows the timing of all SFW events from 1960 to 2010, with the exception of the anomalous event in 2002, determined from NCEP–NCAR reanalysis data. The slope¹ of a least squares linear fit for the timing is $0.383 \text{ day yr}^{-1}$ and it is statistically different from 0 at the 99% confidence level, using a Student’s *t* test. The late years (years of large ozone depletion) and early years (the pre-ozone-hole years) are indicated. The timing of SFW events is later on average in the years of large ozone depletion as compared to the pre-ozone-hole years (the ozone hole cools the polar stratosphere, leading to stronger westerlies in the polar vortex and thus delaying SFW events; e.g., Thompson et al. 2011).

Figure 6 shows the transition in zonal mean zonal wind anomalies (from NCEP–NCAR reanalysis data) averaged from 60° to 70°S for 30 days before and after

¹ This value is less than half that reported by Black and McDaniel (2007b) over the period 1978–2000 but is consistent with the same change in timing over the longer period analyzed here. Thus, the change over the full period is more akin to a step change rather than a sustained linear trend.

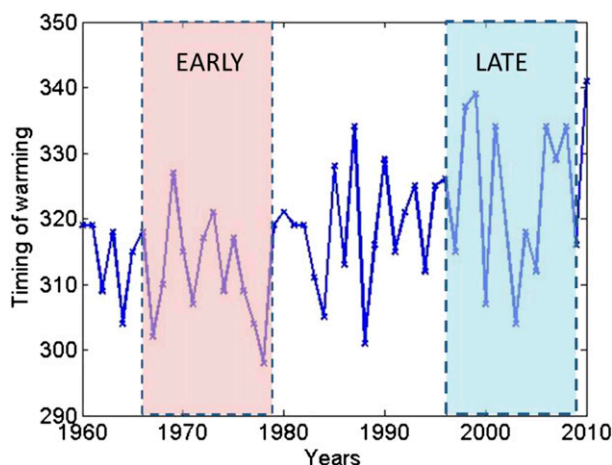


FIG. 5. Timing for SFW events from 1960 to 2010, determined from NCEP–NCAR reanalysis data.

SFW events. Zonal mean zonal wind anomalies are calculated as anomalies from an average seasonal cycle [defined as the sum of the first six Fourier harmonics of a seasonal cycle derived from an annual time series of long-term daily averages; this is also the method used in Black and McDaniel (2007b)]. We note that this method does not eliminate the effects of seasonal changes in annular mode decorrelation time scales (e.g., Baldwin et al. 2003b). Figures 2 (top) and 6 are qualitatively similar. Figure 6 can also be compared with Fig. 3a from Black and McDaniel (2007b), noting that this study used ERA-40 data and analyzed 24 SFW events from 1978 to 2001. In both Figs. 2 (top) and 6, the contours slope downward as the criterion is met first in the stratosphere, after which the effects progress downward with time.

To address the question of whether the influence of stratospheric ozone depletion on surface westerlies is through the delay in timing of SFW events, we examine differences between the years of large ozone depletion and the pre-ozone-hole years. The ozone hole cools the polar stratosphere, changing the north–south temperature gradient, and extending the persistence of the polar vortex (Thompson et al. 2011), leading to SFW events being delayed. Therefore, on the average, SFW events are later in the years of large ozone depletion.

Figure 7 shows composite differences in geopotential height between the late and early years. Geopotential height is shown as anomalies from an average seasonal cycle, as defined earlier in this section. Figure 7a is centered on the average day of occurrence of SFW events for all years, and Fig. 7b has all the years centered on the SFW event day of that year. Daily data smoothed using a centered moving average that averaged data 15 days before and after a given day were used to make this plot.

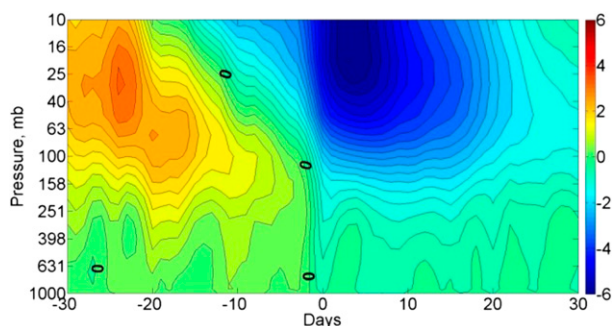


FIG. 6. Transition in zonal mean zonal wind anomalies averaged from 60° to 70°S for a 60-day period centered on SFW events, averaged for 49 SFW events from the NCEP–NCAR reanalysis data. The contour interval is 0.3 m s^{−1}.

In Fig. 7a, the difference in the geopotential anomaly is strongly negative following day 0, and these contours extend all the way to the surface up to 2 months after the mean warming day. Decreases in the geopotential height indicate strengthening of the eastward flow in the polar vortex (corresponding to the high-index polarity of the SAM). Figure 7a is qualitatively similar to Fig. 1b in Thompson et al. (2011), noting that their figure is terminated at 30 hPa and is centered on January, while day 0 in Fig. 7a is 14 November (the average day of occurrence of SFW events). If these signals seen in Fig. 7a are caused purely because of the delayed timing of the final warming, they would disappear in composites where every year is centered on the day where the criterion for SFW is met. The similarity between Figs. 7a and 7b after day 0 leads us to conclude that the tropospheric signal is not being caused by the difference in the timing of final warming events alone. This conclusion is reinforced in Fig. 8. Figure 8 shows the difference in the 850-hPa zonal mean zonal wind (smoothed as in Fig. 7) at 60° (Fig. 8a) and 40°S (Fig. 8b) between the late and early years, centered on the mean warming day (solid line) and the SFW event for each year (dashed line).

The zonal flow is more westerly at 60°S in the late years than in the early years, which corresponds to the high-index polarity of the SAM. Figure 8b shows that the difference is negative at 40°S after the warming (smaller eastward flow). These figures clearly indicate that the difference in surface winds between the late and early years does not change significantly because of the delay in SFW timing.

4. Summary

In the model experiments described here, the imposed seasonal cycle of equilibrium temperature was, by design, confined to the stratosphere. Thus, the tropospheric

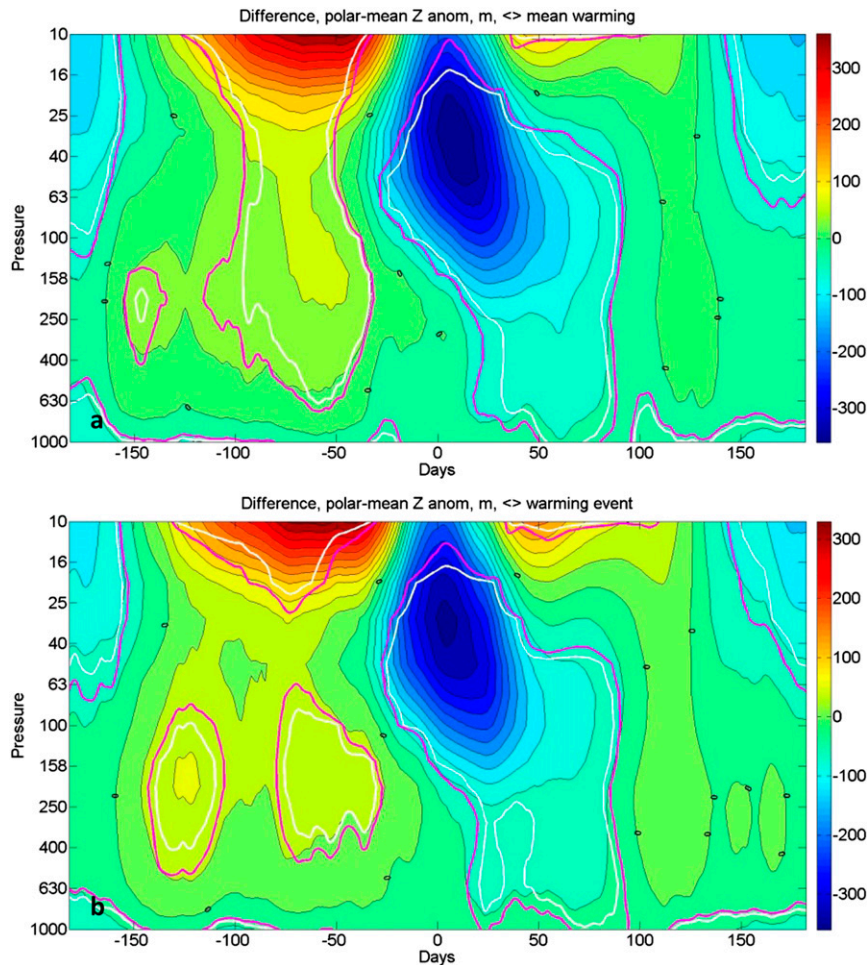


FIG. 7. Polar-mean (averaged from 65° to 90°S) geopotential height, shown as anomalies from an average seasonal cycle (defined as the sum of the first six Fourier harmonics of a seasonal cycle derived from an annual time series of long-term daily averages), difference between the late and early years, centered on (a) the mean warming day and (b) the SFW event. The contour interval is 30 m. Magenta and white contours denote the 90% and 95% confidence intervals for a two-sided *t* test.

signal evident in the model is unambiguously of stratospheric origin and there reinforces the conclusions of Black and McDaniel (2007b) that the tropospheric signal seen in observations is similarly a response to stratospheric events.

Our analysis of data from the NCEP–NCAR reanalysis confirms that there has been a statistically significant shift toward later final warming events in the Southern Hemisphere over the last five decades. This shift, widely attributed to the impact of springtime ozone depletion in the Antarctic lower stratosphere, has been largely coincident with the observed trends in surface winds, which themselves have been attributed to ozone depletion (e.g., Polvani et al. 2011; Thompson et al. 2011). The results of Black and McDaniel (2007b), as well as our simplified model study, indicate that the lower-tropospheric

response to final warming is evident for relatively short time scales (of the order of 10 days), indicating a dynamical response to stratospheric changes rather than a radiative one. These ideas led to the hypothesis that it is the delay in the final warmings that has led to the surface trends. However, since composites made with respect to the variable final warming date show a tropospheric trend that is little changed from those made with respect to calendar date, our results indicate that the surface trends cannot be explained as being caused simply by the trend in the timing of final warming events—that is, it is not simply a matter of the delay of an otherwise unchanged tropospheric response to stratospheric events. That is not to say, of course, that the behavior of the final warming is not responsible for the surface trends: the warmings themselves may have changed in ways other than mere

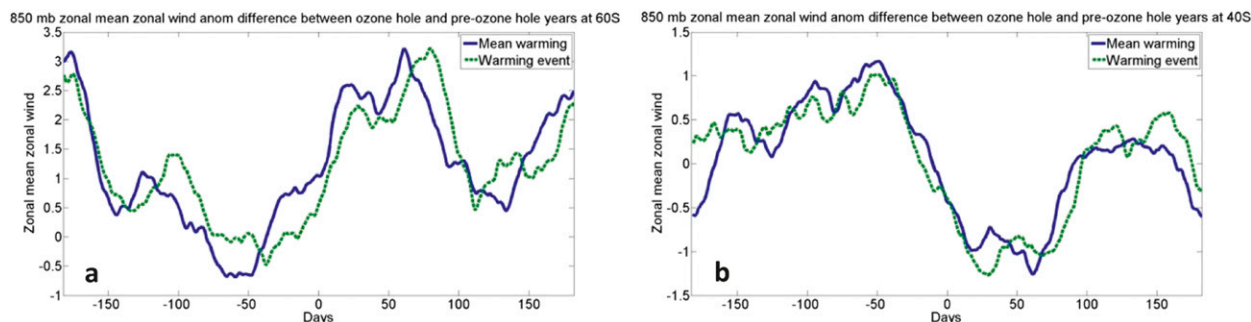


FIG. 8. Difference between the late and early years' 850-hPa zonal mean zonal wind anomaly from the time mean at (a) 60° and (b) 40°S.

timing (and there is some evidence for this). The point is that the trend in the tropospheric signal is not simply a matter of timing.

Acknowledgments. This work has been supported in part by the National Science Foundation. NCEP–NCAR reanalysis data was provided by the NOAA/OAR/ESRL PSD, Boulder, Colorado, from their website at <http://www.esrl.noaa.gov/psd>.

REFERENCES

- Archer, C. L., and K. Caldeira, 2008: Historical trends in the jet streams. *Geophys. Res. Lett.*, **35**, L08803, doi:10.1029/2008GL033614.
- Baldwin, M. P., and T. J. Dunkerton, 2001: Stratospheric harbingers of anomalous weather regimes. *Science*, **294**, 581–584.
- , T. Hirooka, A. O'Neill, S. Yoden, A. J. Charlton, Y. Hio, W. A. Lahoz, and A. Mori, 2003a: Major stratospheric warming in the Southern Hemisphere in 2002: Dynamical aspects of the ozone hole split. *SPARC Newsletter*, No. 20, SPARC Office, Toronto, ON, Canada, 24–26.
- , D. B. Stephenson, D. W. J. Thompson, T. J. Dunkerton, A. J. Charlton, and A. O'Neill, 2003b: Stratospheric memory and skill of extended-range weather forecasts. *Science*, **301**, 636–640.
- Black, R. X., and B. A. McDaniel, 2007a: The dynamics of Northern Hemisphere stratospheric final warming events. *J. Atmos. Sci.*, **64**, 2932–2946.
- , and —, 2007b: Interannual variability in the Southern Hemisphere circulation organized by stratospheric final warming events. *J. Atmos. Sci.*, **64**, 2968–2974.
- , —, and W. A. Robinson, 2006: Stratosphere–troposphere coupling during spring onset. *J. Climate*, **19**, 4891–4901.
- Fogt, R. L., J. Perlwitz, A. J. Monaghan, D. H. Bromwich, J. M. Jones, and J. G. Marshall, 2009: Historical SAM variability. Part II: Twentieth-century variability and trends from reconstructions, observations, and the IPCC AR4 models. *J. Climate*, **22**, 5346–5365.
- Gerber, E. P., and L. M. Polvani, 2009: Stratosphere–troposphere coupling in a relatively simple AGCM: The importance of stratospheric variability. *J. Climate*, **22**, 1920–1933.
- Gillett, N., and D. W. J. Thompson, 2003: Simulation of recent Southern Hemisphere climate change. *Science*, **302**, 273–275.
- Krüger, K., B. Naujokat, and K. Labitzke, 2005: The unusual midwinter warming in the Southern Hemisphere stratosphere, 2002: A comparison to Northern Hemisphere phenomena. *J. Atmos. Sci.*, **62**, 603–613.
- Kushner, P. J., and L. M. Polvani, 2006: Stratosphere–troposphere coupling in a relatively simple AGCM: Impact of the seasonal cycle. *J. Climate*, **19**, 5721–5727.
- Newman, P. A., and E. R. Nash, 2005: The unusual Southern Hemisphere stratosphere winter of 2002. *J. Atmos. Sci.*, **62**, 614–628.
- Polvani, L. M., and P. J. Kushner, 2002: Tropospheric response to stratospheric perturbations in a relatively simple general circulation model. *Geophys. Res. Lett.*, **29**, 1114, doi:10.1029/2001GL014284.
- , D. W. Waugh, G. J. P. Correa, and S.-W. Son, 2011: Stratospheric ozone depletion: The main driver of twentieth-century atmospheric circulation changes in the Southern Hemisphere. *J. Climate*, **24**, 795–812.
- Thompson, D. W. J., and J. M. Wallace, 2000: Annular modes in the extratropical circulation. Part I: month-to-month variability. *J. Climate*, **13**, 1000–1016.
- , and S. Solomon, 2002: Interpretation of recent Southern Hemisphere climate change. *Science*, **296**, 895–899.
- , J. M. Wallace, and G. C. Hegerl, 2000: Annular modes in the extratropical circulation. Part II: Trends. *J. Climate*, **13**, 1018–1036.
- , M. P. Baldwin, and S. Solomon, 2005: Stratosphere–troposphere coupling in the Southern Hemisphere. *J. Atmos. Sci.*, **62**, 708–715.
- , S. Solomon, P. J. Kushner, M. H. England, K. M. Grise, and D. J. Karoly, 2011: Signatures of the Antarctic ozone hole in Southern Hemisphere surface climate change. *Nat. Geosci.*, **4**, 741–749.
- Waugh, D. W., W. J. Randel, S. Pawson, P. A. Newman, and E. R. Nash, 1999: Persistence of the lower stratospheric polar vortices. *J. Geophys. Res.*, **104** (D22), 27 191–27 202.